Nonisothermal Crystallization of Poly(ethylene-*co*-glycidyl methacrylate)/Clay Nanocomposites

Jiann-Wen Huang,[1] Hui-Chuan Hung,[1] Kuo-Shu Tseng,[2] Chiun-Chia Kang[3]

[1]*Department of Styling & Cosmetology, Tainan Woman's College of Arts & Technology, Yung Kang City 710, Taiwan, Republic of China*
[2]*Department of Living Science, Tainan Woman's College of Arts & Technology, Yung Kang City 710, Taiwan, Republic of China*
[3]*R&D Center, Taroko International Co., Ltd., 473 Jong Shan South. Rd., Yung Kang City 710, Taiwan, Republic of China*

Received 8 November 2004; accepted 13 June 2005
DOI 10.1002/app.23199
Published online in Wiley InterScience (www.interscience.wiley.com).

ABSTRACT: The nonisothermal crystallization of poly(ethylene-*co*-glycidyl methacrylate) (PEGMA) and PEGMA/clay were studied by differential scanning calorimeter, at various cooling rates. Avrami model modified by Jeziorny, Ozawa mode and Liu model could successfully describe the nonisothermal crystallization process. Augis–Bennett model, Kissinger model, Takhor model, and Ziabicki model were used to evaluate the activation energy of both samples. It was found that the activation energy of PEGMA/clay nanocomposite was higher than that of neat PEGMA. Experimental results also indicated that the addition of modified clay might retard the overall nonisothermal crystallization process of PEGMA. © 2006 Wiley Periodicals, Inc. J Appl Polym Sci 100: 1335–1343, 2006

Key words: clay; nanocomposite; nonisothermal; crystallization; kinetics

INTRODUCTION

Thermal and mechanical properties can be improved by adding a small fraction of clay to a polymer matrix. These composites exhibit an improved modulus, a lower thermal-expansion coefficient and gas permeability, higher swelling resistance, and enhanced ionic conductivity as compared with those pristine polymers because of the nanoscale structure of the hybrids and the synergism between the polymer and the silicate.[1–10]

Intercalation of layered silicates has been proven to be a versatile approach to prepare a nanocomposite. The preparation involves intercalation of a suitable monomer and exfoliating the layered galleries into their nanoscale elements by subsequent polymerization. However, this method requires a proper monomer or solvent as a medium, and such requirement puts a strong restraint on the selection of polymers used for the composites. Many nanocomposites based on polar polymers, such as epoxide polymer[11,12] and poly(ethylene oxide) (PEO),[13,14] have been successfully prepared with intercalation technique. These polar polymers are much more successful due to the fact that they can be intercalated between smetic layers of the clay, from which the nanocomposite is derived.[15–18]

Correspondence to: J.-W. Huang (jw.huang@msa.hinet.net).

Journal of Applied Polymer Science, Vol. 100, 1335–1343 (2006)

Some researchers prepared nanocomposites by direct melt blending in a twin-screw extruder using maleic anhydride graft polypropylene[16–21] and polyethylene.[22] In our previous article, nanocomposites based on poly(ethylene-*co*-glycidyl methacrylate) (PEGMA) and commercial modified clay had been successfully prepared via direct melt intercalation, and the isothermal crystallization process was also studied.[23] In this paper, nonisothermal crystallization of PEGMA and PEGMA/Clay nanocomposite were both studied by DSC, and several nonisothermal crystallization models were used to describe the crystallization process. In addition, the activation energies of crystallization were also estimated by Augis–Bennett model, Kissinger model, and Takhor model.

EXPERIMENTAL

Materials

Commercial grade PEGMA (CG5004) was supplied by Sumitomo Chemical Co Ltd. (Tokyo, Japan), which contains 81 wt % ethylene and 19 wt % glycidyl methacrylate. Commercial modified montmorillonite clay was purchased from Vulchem (Trade Name : KH-γc; Taipei, Taiwan). Both materials were used as received without further purification.

Sample preparation

All materials were dried at room temperature in a vacuum oven for 6 h before compounding. PEGMA

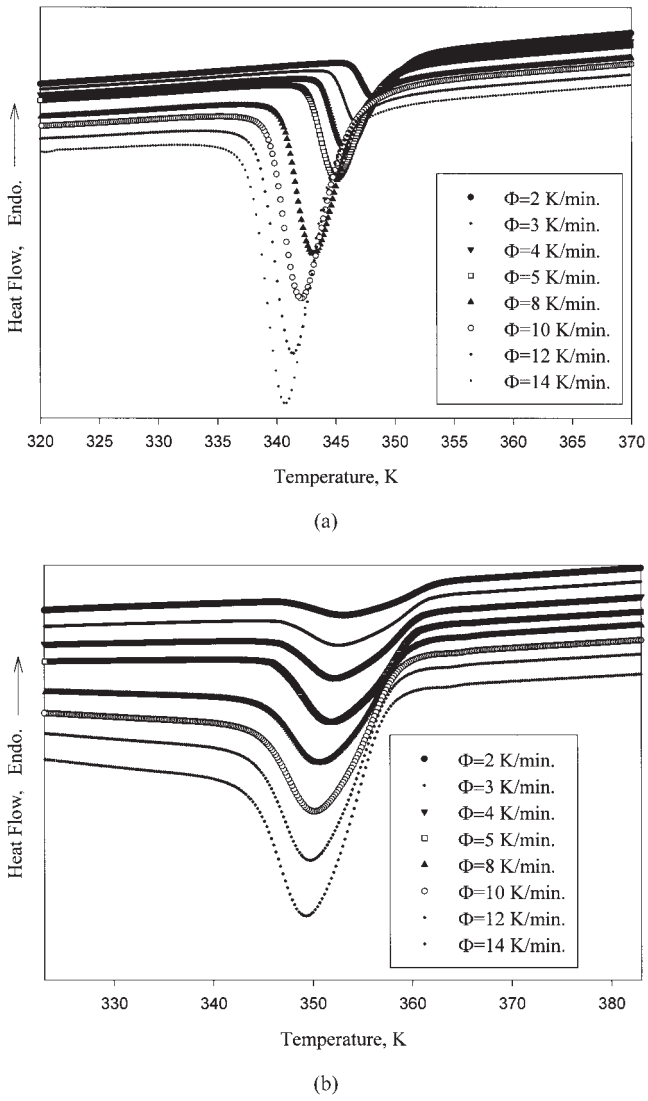

Figure 1 DSC nonisothermal measurement curves for PEGMA and PEGMA/clay nanocomposite. (a) PEGMA; (b) PEGMA/clay.

and 20 wt % modified clay were compounded with twin-screw extruder (Continent Machinery Company, Model CM- MTE; Tainan, Taiwan) at 453 K and 300 rpm to make a masterbatch. The masterbatch was then mixed with PEGMA and re-compounded at 433 K and 300 rpm conditions to prepare 3 wt % nanocomposite (PEGMA/clay).[23] The neat PEGMA went through the same thermal history as PEGMA/clay for comparison.

Nonisothermal crystallization

The nonisothermal crystallization behaviors of polymer composite were investigated with a differential scanning calorimeter, Perkin–Elmer DSC-1. The differential scanning calorimeter was calibrated using indium with samples weights of 8–10 mg. All operations were carried out in a nitrogen atmosphere. Before the data gathering, the samples were heated to 393 K and held at this temperature in molten state for 5 min to eliminate the influence of thermal history. The sample melts were then subsequently cooled to 308 K at a cooling rate of 2, 3, 4, 5, 8, 10, 12, and 14 K/min respectively.

RESULTS AND DISCUSSION

The crystallization processes of PEGMA and PEGMA/clay nanocomposite were measured at a range of cooling rates from 2 to 14 K/min. The DSC curves of the samples were compared in Figure 1. The cooling rate dependences of the onset (T_o) and peak (T_p) temperatures of the crystallization exotherms were shown in Table I. In both samples, the T_o and T_p shifted to a lower temperature with increasing cooling rate, which indicated that the lower the cooling rate, the earlier the crystallization starts. For a given cooling rate, T_o and T_p of PEGMA/Clay were higher than that of neat PEGMA because modified clay acted as nucleating agent and therefore PEGMA in PEGMA/clay nanocomposites started to crystallize earlier. However, the crystallization peak width of PEGMA/clay [Fig. 1(b)] was broader than that of neat PEGMA [Fig. 1(a)], which indicated that PEGMA/clay needed more time to complete the crystallization; that is, the addition of modified clay retarded the crystallization.

TABLE I
Characteristic Data of Nonisothermal Melt Crystallization Exotherms for PEGMA and PEGMA/Clay

Cooling rate Φ, K/min	PEGMA			PEGMA/clay		
	T_o (K)	T_p (K)	$t_{1/2}$ (min)	T_o, (K)	T_p (K)	$t_{1/2}$ (min)
2	351.7	348.3	1.83	362.9	352.6	4.18
3	351.0	347.0	1.40	361.7	352.2	2.59
4	350.9	345.9	1.16	361.3	351.9	1.96
5	349.6	345.1	0.87	360.7	351.5	1.54
8	348.5	343.2	0.63	359.3	350.6	0.94
10	347.7	342.0	0.53	358.8	350.1	0.77
12	346.7	341.4	0.44	358.3	349.6	0.63
14	345.6	340.8	0.34	357.7	349.3	0.57

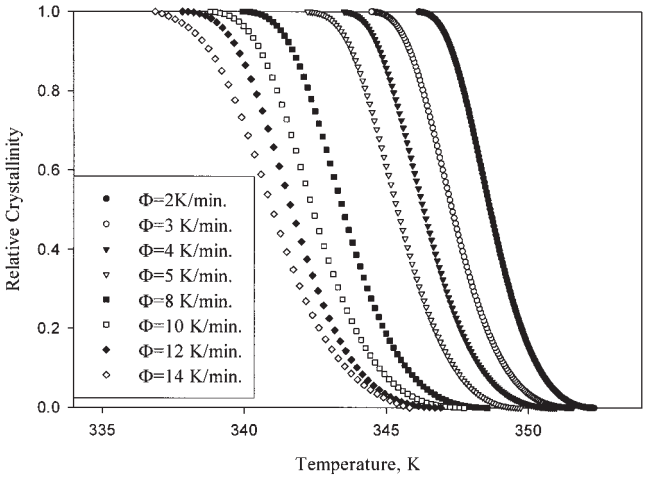

(a)

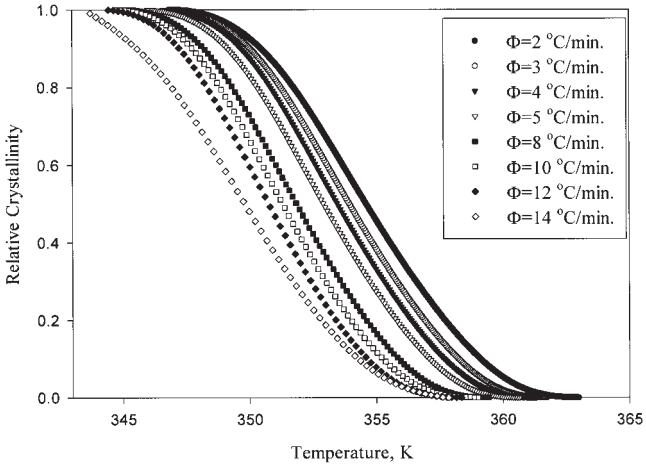

(b)

Figure 2 Experimental relative crystallinity as a function of temperature at different cooling rate. (a) PEGMA; (b) PEGMA/clay.

The relative crystallinity as a function of temperature, X_T, was calculated as the ratio of the exothermic peak areas[24–26]:

$$X_T = \frac{\int_{T_0}^{T} \left[\frac{dH_c}{dT}\right] dT}{\int_{T_o}^{T_\infty} \left[\frac{dH_c}{dT}\right] dT} \quad (1)$$

where T is an arbitrary temperature, dH_c is the enthalpy of crystallization released during an infinitesimal temperature interval dT; Figures 2(a) and 2(b) present the relative crystallinity (X_t) as a function of temperature for PEGMA and PEGMA/clay nanocomposite. During the nonisothermal crystallization process, the time, t, and temperature exhibit the following relationship:

$$t = \left|\frac{T_o - T}{\Phi}\right| \quad (2)$$

where Φ is cooling rate. The abscissa of temperature in Figures 2(a) and 2(b) could be transformed into a timescale. The relative crystallinity (X_t) of PEGMA and PEGMA/clay nanocomposite as a function of time were illustrated in Figures 3(a) and 3(b). It can be seen clearly from Figures 3(a) and 3(b) that the higher the cooling rate, the shorter the time for completing the crystallization.

The half-time of nonisothermal crystallization, $t_{1/2}$, can be obtained from the following relationship:

$$t_{1/2} = |T_o - T_{1/2}|/\Phi \quad (3)$$

where $T_{1/2}$ is the temperature at which $X_t = 50\%$ and Φ is the cooling rate. Table I also shows the $t_{1/2}$ for PEGMA and PEGMA/clay. The inverse value of $t_{1/2}$

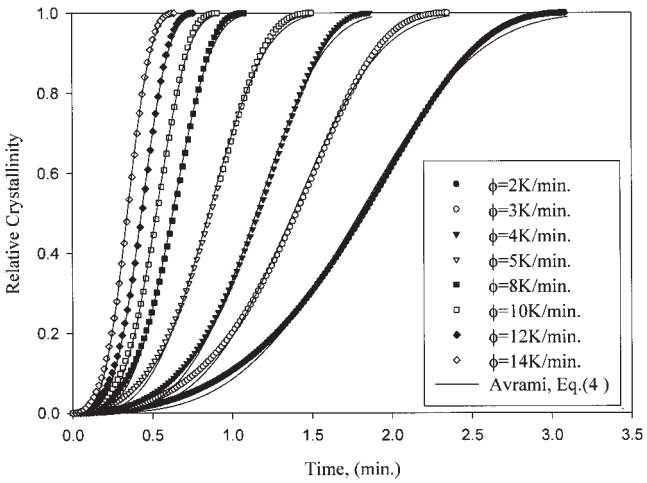

(a)

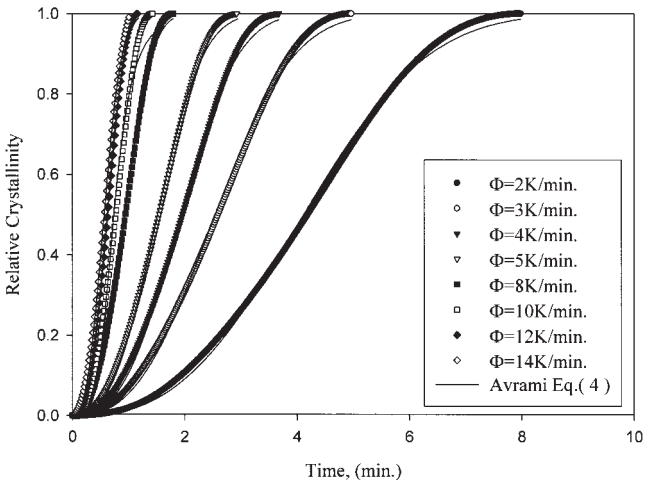

(b)

Figure 3 Experimental relative crystallinity as a function of time at different cooling rate. (a) PEGMA; (b) PEGMA/clay.

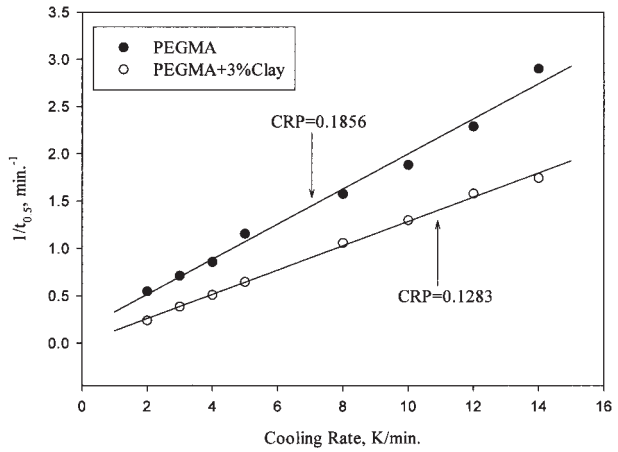

Figure 4 Plots of reciprocal half-time of crystallization as a function of cooling rate for PEGMA and PEGMA/clay.

(i.e., $1/t_{1/2}$) signifies the bulk crystallization rate. The higher the $t_{1/2}$ value (i.e., lower $1/t_{1/2}$ value), the slower the crystallization was. The $t_{1/2}$ value decreased with increasing cooling rate, indicating that the polymer crystallized faster when the cooling rate was increased. At given cooling rate, the value of $t_{1/2}$ for neat PEGMA was lower than that for PEGMA/clay, signifying that the addition of modified clay decreased the overall crystallization process. The overall crystallization rate is governed by nucleation and diffusion.[27] As mentioned previously, the addition of modified clay acted as nucleating agent leading to an increase in nucleation rate, onset, and peak temperatures; however, the modified clay also hindered the crystallization under nonisothermal conditions.[28–31]

The crystallization rate parameter (CPR)[32,33] is used to quantitatively compare nonisothermal crystallization rate, which can be determined from the slope of a line drawn through a plot of $1/t_{1/2}$ versus the cooling rate. The faster the crystallization rate, the higher the slope is. Figure 4 shows plots of $1/t_{1/2}$ as a function of cooling rate. The CRP (0.1856) of neat PEGMA was higher than that (0.1283) of PEGMA/clay nanocomposite, indicating that neat PEGMA crystallized at a higher rate than PEGMA in PEGMA/clay nanocomposite.

Avrami model

Avrami equation[33–43] can be used to describe the primary stage of nonisothermal crystallization. The Avrami equation is expressed as follows:

$$X_t = 1 - exp(-(K_a t)^{n_a}) \tag{4}$$

where X_t is the relative crystallinity, t is crystallization time, K_a is the Avrami crystallization rate constant, and n_a is the Avrami exponent. X_t can be calculated as the ratio between the area of the exothermic peak at time t and the total measured area of crystallization. Values of K_a and n_a were obtained by fitting experimental data of X_t into eq. (4) and the results were shown in Table II.

Avrami equation is usually written as following:

$$X_t = 1 - exp(-k_a^* t^{n_a^*}) \tag{5a}$$

or

$$\ln[-\ln(1-X_t)] = \ln k_a^* + n_a^* \ln t \tag{5b}$$

Values of k_a and n_a could be determined from the slope (X_t = 0.1–0.8) and intercept with the y axis by plotting $\ln[-\ln(1-X_t)]$ versus $\ln(t)$ as shown in Figure 5 and the results were also shown in Table II for

TABLE II
Avrami Kinetics Parameters

Sample	Cooling rate (K/min)	n_a	K_a	K_j	R^2	n_a^*	k_a^*	R^2
PEGMA	2	3.48	0.5002	0.7072	0.9992	3.20	0.1042	0.9985
	3	3.63	0.6535	0.8678	0.9993	3.35	0.2299	0.9972
	4	3.83	0.7901	0.9428	0.9993	3.55	0.4159	0.9972
	5	3.45	1.0535	1.0105	0.9994	3.21	1.1350	0.9974
	8	3.71	1.4436	1.0470	0.9995	3.47	3.4452	0.9974
	10	3.73	1.7254	1.0561	0.9995	3.50	6.5339	0.9974
	12	3.66	2.0923	1.0635	0.9996	3.47	12.6038	0.9977
	14	3.40	2.6100	1.0709	0.9997	3.27	22.6011	0.9983
PEGMA/ Clay	2	2.74	0.2126	0.4611	0.9993	2.52	0.0193	0.9986
	3	2.68	0.3432	0.7001	0.9991	2.44	0.0702	0.9982
	4	2.78	0.4547	0.8212	0.9992	2.54	0.1296	0.9984
	5	2.75	0.5768	0.8958	0.9992	2.52	0.2391	0.9984
	8	2.80	0.9441	0.9928	0.9993	2.58	0.4528	0.9986
	10	2.92	1.1614	1.0151	0.9994	2.72	1.4508	0.9988
	12	2.93	1.4137	1.0293	0.9995	2.72	2.4870	0.9988
	14	2.63	1.5409	1.0314	0.9992	2.46	2.8123	0.9982

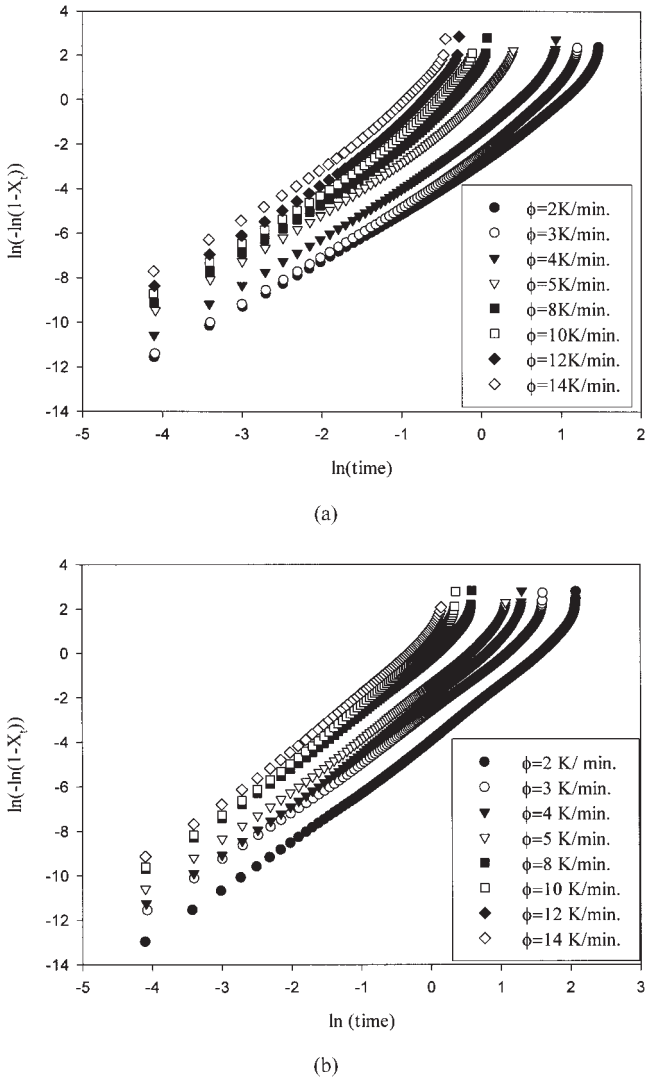

Figure 5 Avrami analysis from eq.(5b) for PEGMA and PEGMA/Clay. (a) PEGMA; (b) PEGMA/clay.

comparison. K_a is more preferable than k_a because it is independent of Avrami exponent and its dimension is given in $(\text{time})^{-1}$.[44–46]

In nonisothermal crystallization, K_a and n_a do not have the same physical significance as in the isothermal crystallization because under nonisothermal crystallization, the temperature changes constantly. This temperature changes affects the rate of both nuclei formation and spherulite growth. However, eq. (4) provided a good fit to experimental data, according to the regression coefficient (R^2) and Figure 3.

To meet the requirement of Avrami model, Jeziorny[47] assumed constant or approximately constant cooling rate and proposed the final form of the parameter characterizing the kinetics of nonisothermal crystallization:

$$\ln K_j = \frac{\ln K_a}{\Phi} \tag{6}$$

The values of K_J were listed in Table II. It was found that K_J increased with increasing cooling rate for both neat PEGMA and PEGMA/clay nanocomposite. At the same cooling rate, K_J of PEGMA/clay nanocomposite was lower than that of PEGMA, indicating that the addition of modified clay might hinder the crystallization under nonisothermal conditions.

Ozawa model

Ozawa extended the Avrami theory from isothermal crystallization to the nonisothermal crystallization by assuming that crystallization occurs at a constant cooling rate and the equation is as following[48,49]:

$$X_T = 1 - \exp\left[-\left(\frac{K_o}{\Phi}\right)^{n_o}\right] \tag{7}$$

Where K_o and n_o are Ozawa crystallization rate constant and Ozawa exponent, respectively. Figure 6 illustrates the plots of $\ln[-\ln(1 - X_t)]$ as a function of $\ln \Phi$ for a fixed temperature. The K_o and n_o could be estimated from the y-intercept [($K_o = \exp(y\text{-intercept}/n_o)$) and slope. The Ozawa kinetic parameters as well as regression coefficient (R^2) were listed in Table III. Based on the Figure 6 and regression coefficient (R^2) listed in Table III, it is suggested that Ozawa model provided a satisfactorily good fit to the experimental data of both samples studied. Ozawa exponent n_o was found to range from 3.12 to 3.63 for neat PEGMA within 340–348 K, and from 0.68 to 1.25 for PEGMA/clay within 348–356 K. n_o Increased with increasing crystallization temperature, indicating the change of nucleation during the crystallization process.[50,51] The Ozawa crystallization rate constant K_o, was found to show a reduction with increasing temperature, suggesting that PEGMA displayed a slower crystallization rate with increasing temperature.

Liu model

Liu et al. [52] combined the Avrami model and Ozawa model to deal with the nonisothermal crystallization behavior, and its form is given as follow:

$$\ln \Phi = \ln\left[\frac{K_o^{n_o}}{K_a^{n_a}}\right]^{\frac{1}{n_o}} - \frac{n_a}{n_o}\ln t \tag{8a}$$

$$F(T) = \left[\frac{K_o^{n_o}}{K_a^{n_a}}\right]^{\frac{1}{n_o}} \tag{8b}$$

$$a = \frac{n_a}{n_o} \tag{8c}$$

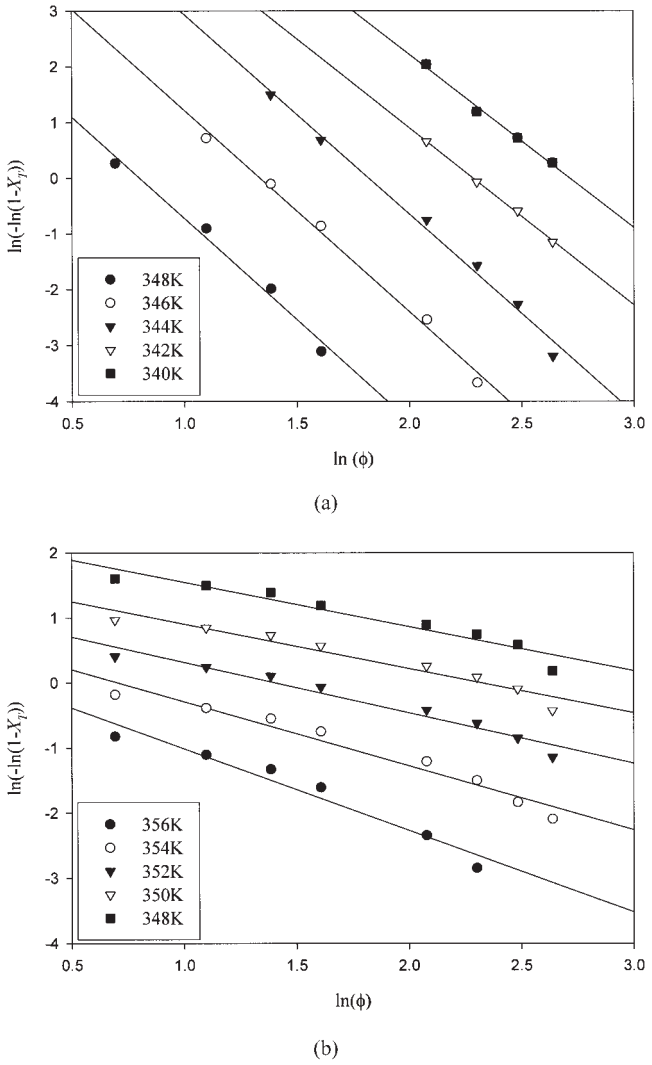

Figure 6 Ozawa analysis based on the nonisothermal crystallization of PEGMA and PEGMA/clay (a) PEGMA; (b) PEGMA/clay.

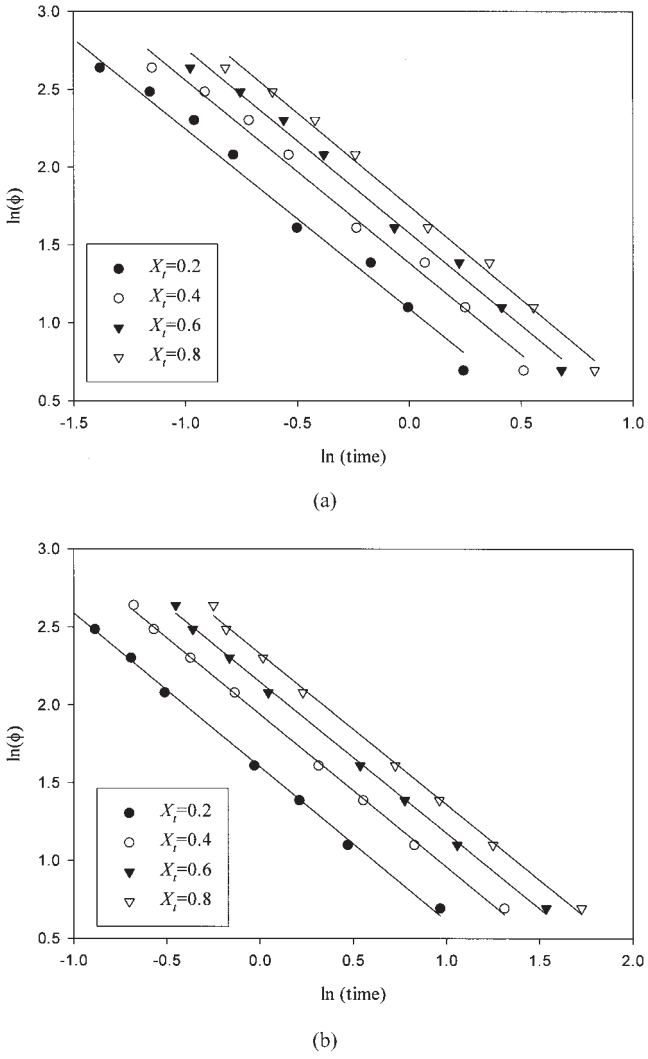

Figure 7 Plots of ln Φ; verus ln t for different relative degree of crystallinity for PEGMA and PEGMA/clay (a) PEGMA; (b) PEGMA/clay.

Where the kinetic parameter, $F(T)$, refers to the value of the cooling rate, which has to be chosen at the unit crystallization time when the measured system amounts to a certain degree of crystallinity; a is the Avrami exponent (n_a) to the Ozawa exponent (n_o). At a given degree of crystallinity, plotting ln Φ versus ln t (Fig. 7) yielded a linear relationship between ln Φ and ln t and the values of $F(t)$ and a could be obtained from the slopes and intercepts of these lines, respectively, listed in Table IV. The value of a varies from 1.18 to 1.20 for neat PEGMA and 0.97 to 0.99 for PEGMA/clay nanocomposite. The value of $F(T)$ increased with increasing degree of crystallinity, indicating that at unit crystallization time, a higher cooling rate should be applied to reach a higher degree of crystallinity. At the same relative degree of crystallinity, the value of $F(T)$ for PEGMA/clay nanocomposite was higher than that of neat PEGMA, that is, to reach the same relative degree of crystallinity, PEGMA/clay nanocomposite required higher cooling rate, which indicated that PEGMA/clay nanocomposite crystallized at a slower rate than neat PEGMA.

TABLE III
Ozawa Kinetics Parameters

Sample	Temperature (K)	n_o	K_o	R^2
PEGMA	340	3.12	15.98218	0.9861
	342	3.19	9.862254	0.9928
	344	3.58	6.181175	0.9908
	346	3.62	3.806615	0.9984
	348	3.63	2.131924	0.9987
PEGMA/Clay	348	0.68	26.56014	0.9308
	350	0.68	10.37818	0.9426
	352	0.78	4.070827	0.9575
	354	0.98	2.041685	0.9594
	356	1.25	1.214679	0.9540

TABLE IV
Value of *F*(*T*) and *a* for PEGMA and PEGMA/CIay

Sample	X_t	$F(T)$	a	R^2
PEGMA	0.2	2.94	1.20	0.9875
	0.4	3.99	1.18	0.9890
	0.6	4.84	1.19	0.9912
	0.8	5.74	1.19	0.9932
PEGMA/Clay	0.2	4.96	0.99	0.9983
	0.4	6.96	0.98	0.9987
	0.6	8.57	0.97	0.9983
	0.8	10.28	0.97	0.9977

Ziabicki analysis

Ziabicki[53–55] suggested that the kinetics of polymer phase transformation can be described by a first-order kinetic equation:

$$\frac{dX_t}{dt} = K_z(1 - X_t) \tag{9}$$

where X_t is the relative degree of crystallinity as a function of time and K_z is a temperature-dependent crystallization rate function. Ziabicki suggested a concept of kinetic crystallinity as follows:

$$G = \int_{T_g}^{T_m} K_z dT \tag{10}$$

The kinetic crystallizability, G, characterizes the degree of crystallinity obtained when the polymer is cooled at unit cooling rate from the melting temperature (T_m) to the glass transition temperature (T_g). Jeziorny[34,47] derived a simple equation to calculate the kinetic crystallizability, G:

$$G = \int_{T_g}^{T_m} K_z \, dT = \left(\frac{\pi}{\ln 2}\right)^{1/2} K_{z,max}\frac{D}{2} \tag{11}$$

where $K_{z,\max}$ is the value of K_z at the maximum crystallization rate, and D is the half-with of the crystallization curve.

In nonisothermal crystallization, crystallization rate function K_z is replaced with a derivation function of the relative crystallinity, $(dX/dT)_\Phi$, specific for each cooling rate. Equation[10] is replaced by[33,35]

$$G_\varphi = \int_{T_g}^{T_m} (dX/dT)_\Phi \, dT = \left(\frac{\pi}{\ln 2}\right)^{1/2} (dX/dT)_{\Phi,max}\frac{D_\Phi}{2} \tag{12}$$

where $(dX/dT)_{\Phi,\max}$ is the maximum crystallization rate, and D_Φ is the half-with of the derivative relative crystallinity as a function of temperature. G_Φ is the kinetic crystallizability at an arbitrary cooling rate, Φ. Because of the effect of cooling rate, G_Φ must be corrected properly as follows:

$$G_c = \frac{G_\Phi}{\Phi} \tag{13}$$

After normalizing the effect of the cooling rate, the values of kinetic crystallizability at the unit cooling G_c are shown in Table V. Since the physical meaning of the G_c parameter is to characterize the ability of a polymer to crystallize when it is cooled from the melting temperature to the glass transition temperature at unit cooling rate, the higher the G_c value, the more readily the polymer crystallizes. As shown in Table V, PEGMA/clay nanocomposite had a lower value of $G_{c,,}$ which indicated the nanocomposite had a lower crystallize rate. The results are similar to the afore-mentioned other models.

Comparison of kinetic models

All these four models (Avrami, Ozawa, Liu, and Ziabicki) provided good fits to experimental data and

TABLE V
Characteristic Data of Nonisothermal Melt Crystallization Exotherms for PEGMA and PEGMA/Clay

	Cooling rate (K/min)							
	2	3	4	5	8	10	12	I4
PEGMA								
D_Φ (K)	3.16	3.43	3.28	3.41	3.67	3.77	3.81	3.95
$(dX/dT)_{\Phi\ \max}$	0.67	0.91	1.26	2.1	2.77	3.1	3.47	3.95
G_Φ	2.25	3.32	4.40	7.62	10.82	12.43	14.07	16.60
G_c	1.13	1.11	1.10	1.52	1.35	1.24	1.17	1.19
$T_{\max}$ (K)	348.37	347.00	345.96	345.05	343.09	342.02	341.32	340.65
PEGMA + 3% Clay								
D_Φ (K)	8.51	8.46	8.25	8.36	8.41	8.4	8.6	9.1
$(dX/dT)_{\Phi\ \max}$	0.22	0.35	0.47	0.6	0.99	1.27	1.42	1.57
G_Φ	1.99	3.15	4.13	5.34	8.86	11.35	12.99	15.20
G_c	1.00	1.05	1.03	1.07	1.11	1.14	1.08	1.09
$T_{\max}$ (K)	353.81	353.09	352.57	352.12	351.14	350.74	350.07	349.33

the kinetic parameters from these models (K_J, K_o, $F(T)$, and G_c) predicted correctly that the crystallization rate of PEGMA was greater than that of PEGMA/CIay. It is difficult, however, for Ozawa, Liu, and Ziabicki models to reconstruct the nonisothermal crystallization process (e.g. Fig. 3) with those kinetic parameters. Avrami model, on the other hand, has provided a simple method to describe a nonisothermal crystallization process although the physical meanings of its kinetic parameters (K_a and n_a) are not yet clear. To be able to simulate a nonisothermal process is of great interest because industrial operations involve mostly nonisothermal crystallization. Avrami model, with the highest R^2 value, also provided the best fit among the four models.

Crystallization activation energy

To estimate the effective energy barrier (ΔE) for nonisothermal melt crystallization process, many models[56–58] were proposed to estimate the crystallization activation energy from nonisothermal thermo analytical investigations. Considering the influence of the various cooling rate in the nonisothermal crystallization with the peak temperature (T_p), the activation energy ΔE could be determined as following:

1. Augis–Bennett model[56]

$$\frac{d\{\ln[\Phi/(T_o - T_p)]\}}{d(1/T_p)} = -\frac{\Delta E}{R} \tag{14}$$

2. Kissinger model[57]

$$\frac{d[\ln(\Phi/T_p^2)]}{d(1/T_p)} = -\frac{\Delta E}{R} \tag{15}$$

3. Takhor model[58]

$$\frac{d[\ln(\Phi)]}{d(1/T_p)} = -\frac{\Delta E}{R} \tag{16}$$

where R is the universal gas constant. Figures 8(a)–8(c) show the plot of Augis–Bennett model, Kissinger model, and Takhor model, respectively. The activation energy ΔE can be calculated from the slopes ($-\Delta E/R$) of these plots and the results are listed in Table VI. ΔE is the activation energy required to transport molecular segments to the crystallization surface. The higher the ΔE value, the lower the crystallization ability of the polymer becomes. The three models all showed that PEGMA/clay nanocomposite had a higher value of ΔE than that of neat PEGMA, which indicated the nanocomposite had a lower crystallize rate.

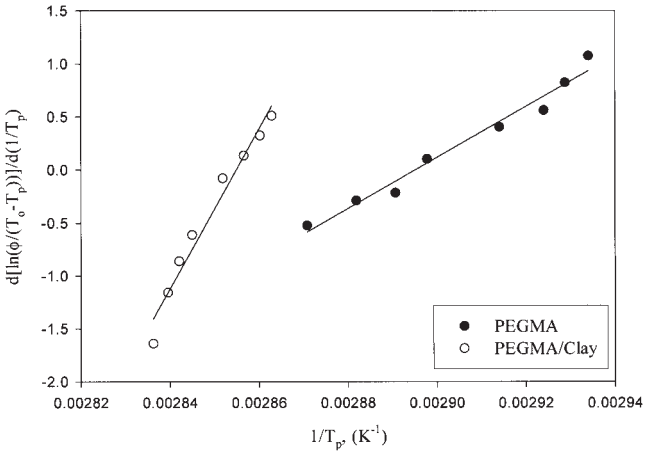

(a)

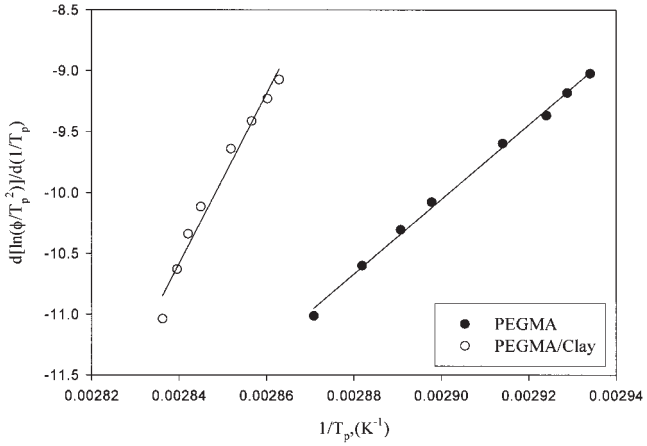

(b)

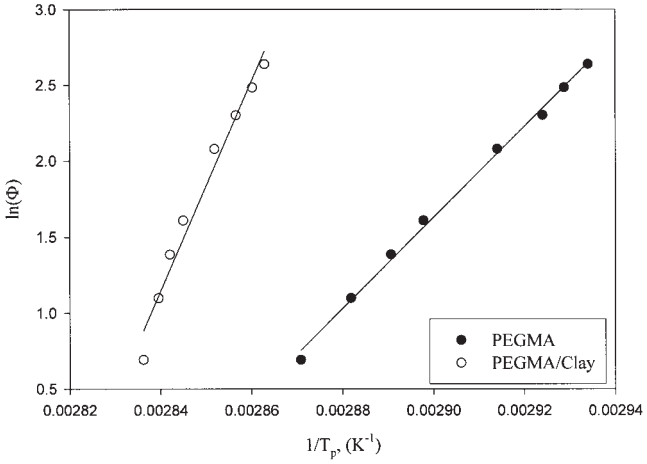

(c)

Figure 8 Determination of the crystallization activation energy for PEGMA and PEGMA/clay (a) Augis–Bennett model; (b) Kissinger model; and (c) Takhor model.

CONCLUSIONS

The investigation of nonisothermal crystallization kinetics of neat PEGMA and PEGMA/clay nanocom-

TABLE VI
Crystallization Activation Energy ΔE (kJ/mole) Calculated from Augis–Bennett, Kissinger, and Takhor Models

	Samples	
	PEGMA	PEGMA/Clay
Augis–Bennett	−199.57	−625.66
Kissinger	−254.57	−579.04
Takhor	−248.84	−573.20

posite were carried out by DSC. The $t_{1/2}$ and CRP showed that the crystallization rate of PEGMA was higher than that of PEGMA/clay nanocomposite at a given cooling rate. Avrami model modified by Jeziorny, Ozawa modem, and Liu model could successfully describe the nonisothermal crystallization process. All rate parameters suggested that neat PEGMA crystallizes faster than PEGMA/clay nanocomposite. The ability for PEGMA to crystallize from the molten state under a unit cooling rate under Ziabicki's model, from which it was found that PEGMA/clay nanocomposite had a lower value of G_c, which indicate the nanocomposite has a lower crystallize rate than neat PEGMA. The energy barrier of governing the nonisothermal melt-crystallization based on Augis–Bennett model, Kissinger model, and Takhor model, all showed PEGMA/clay nanocomposite had a higher value of ΔE than that of neat PEGMA, which indicated the nanocomposite has a lower crystallize rate.

References

1. Whiteside, G. M.; Mathias, T. P.; Seto, C. T. Science 1991, 254, 1312.
2. Gleiter, H. Adv Mater (Weinheim, Ger) 1992, 4, 474.
3. Novak, B. Adv Mater (Weinheim, Ger) 1993, 5, 422.
4. Messersimith, P. B.; Giannelis, E. P. J Polym Sci Part A: Polym Chem 1995, 33, 1047.
5. Usuki, A.; Kawasumi, T.; Kojima, M.; Fukushima, Y.; Okada, A. J Mater Res 1993, 8, 1179.
6. Kojima, Y.; Usuki, A.; Kawasumi, M.; Fukushima, Y.; Okada, A.; Kurauchi, T. J Mater Res 1993, 8, 1185.
7. Yano, K.; Usuki, A.; Okada, A.; Kurauchi, T.; Kamigato, O. J Polym Sci Part A: Polym Chem 1993, 31, 2493.
8. Wang, K. H.; Choi, M. H.; Koo, C. M.; Choi, Y. S.; Chung, I. J Polym Sci 2001, 42, 9819.
9. Fukushima, Y.; Okada, A.; Kawasumi, M.; Kurauchi, T.; Kamigaito, O. Clay Miner 1988, 23, 27.
10. Giannelis, E. P. Adv Mater (Weinheim, Ger) 1996, 8, 29.
11. Wang, M. S.; Pinnavaia, T. J. Chem Mater 1994, 6, 468.
12. Messersmith, P. B.; Giannelis, E. P. Chem Mater 1994, 6, 1719.
13. Vaia, R. A.; Ishii, H.; Giannelis, E. P. Chem Mater 1993, 5, 1694.
14. Vaia, R. A.; Vasudevan, S.; Krawiec, W.; Scanlon, L. G.; Giannelis, E. P. Adv Mater (Weinheim, Ger) 1995, 7, 154.
15. Chin, I. J.; Albrecht, T. T.; Kim, H. C.; Russella, T. P.; Wang, J. Polymer 2001, 42, 5947.
16. Kaempfer, D.; Thomann, R.; Mohlhaupt, R. Polymer 2002, 43, 2909.
17. Reichert, P.; Nitz, H.; Klinke, S.; Brandsch, R.; Thomann, R.; Mulhaupt, R. Macromol Mater Eng 2000, 275, 8.
18. Zanetti, A. U.; Camino, G.; Canavese, D.; Morgan, A. B.; Lamelas, F. J.; Wilkie, C. A. Chem Mater 2002, 14, 189.
19. Kawasumi, M.; Hasegawa, N.; Kato, M.; Usuki, A.; Okada, A. Macromolecules 1997, 30, 6333.
20. Hasegawa, N.; Kawasumi, M.; Kato, M.; Usuki, A.; Okada, A. J Appl Polym Sci 1998, 67, 87.
21. Adams, T.; Oliver, W.; Martina, M. P.; Manfred, P. H.; Bernhard, S. Polym Degrad Stab 2003, 82, 133.
22. Liang, G.; Xu, J.; Bao, S.; Xu, W. J Appl Polym Sci 2004, 91, 3974.
23. Huang, J. W.; Kang, C. C. J Appl Polym Sci, submitted.
24. Hay, J. N.; Sabir, M. Polymer 1969, 10, 203.
25. Hay, J. N.; Fitzgerald, P. A.; Wiles, M. Polymer 1976, 17, 1015.
26. Hay, J. N. Br Polym J 1979, 11, 137.
27. Fatou, J. G. Makromol Chem 1984, 7, 131.
28. Zhang, G.; Yan, D. J Appl Polym Sci 2003, 88, 2181.
29. Ma, C. C.; Kuo, C. T.; Kuan, H. C.; Chiang, C. L. J Appl Polym Sci 2003, 88, 1686.
30. Jimenez, C. G.; Ogata, N.; Kawai, H.; Ogihara, T. J Appl Polym Sci 1997, 64, 2211.
31. Weng, W.; Chen, G.; Wu, D. Polymer 2003, 44, 8119.
32. Zhang, U.; Zheng, H.; Lou, X.; Ma, D. J Appl Polym Sci 1994, 51, 51.
33. Supaphol, P.; Dangseeyun, N.; Srimoaon, P. Polym Test 2004, 23, 175.
34. Supaphol, P. J Appl Polym Sci 2000, 78, 338.
35. Supaphol, P.; Dangseeyun, N.; Srimoaon, P.; Nithitanakul, M. Thermochim Acta 2003, 406, 207.
36. Vyazovkin, S.; Sbirrazzuoli, N. J Phys Chem B 2003, 107, 882.
37. Kolmogorov, A. N.; Akad, I. Nauk USSR Ser Mater 1937, 1, 355.
38. Johnson, W. A.; Mehl, K. F. Trans Am Inst Min Metall Pet Eng 1939, 135, 416.
39. Avrami, M. J Chem Phys 1939, 7, 1103.
40. Avrami, M. J Chem Phys 1940, 8, 212.
41. Avrami, M. J Chem Phys 1941, 9, 177.
42. Evans, U. R. Trans Faraday Soc 1945, 41, 365.
43. Ding, Z. J.; Spruiell, E. J Polym Sci Part B: Polym Phys 1997, 35, 1077.
44. Supaphol, P.; Spruiell, J. E. Polymer 2001, 42, 699.
45. Wunderlich, B. Macromolecular Physics, Vol. 2; Academic Press: New York, 1976.
46. Supaphol, P. Thermochim Acta 2001, 170, 37.
47. Jeziorny, A. Polymer 1978, 19, 1142.
48. Ozawa, T. Polymer 1971, 12, 150.
49. Apiwanthanakorn, N.; Supaphol, P.; Nithitanakul, M. Polym Test 2004, 23, 817.
50. Qiu, Z.; Fujinami, S.; Komura, M.; Nakajima, K.; Ikehara, T.; Nishi, T. Polym J 2004, 36, 642.
51. Somrang, N.; Nithitanakul, M.; Grady, B. P.; Supaphol, P. Euro Polym J 2004, 40, 829.
52. Liu, T. X.; Mo, Z. S.; Wang, S. E.; Zhang, H. F. Polym Eng Sci 1997, 37, 568.
53. Ziabicki, A. Colloid Polym Sci 1974, 252, 433.
54. Ziabicki, A. J Chem Phys 1968, 48, 4368.
55. Ziabicki, A. Appl Polym Symp 1967, 6, 1.
56. Augis, J. A.; Bennett, J. E. J Ther Anal 1978, 13, 283.
57. Kissinger, H. E. J Res Natl Bur Stand 1956, 57, 217.
58. Takhor, R. L. Advances in Nucleation and Crystallization of Glasses; American Ceramics Society: Columbus, 1971; p 166.